

Glaciological observations at Dome Argus, East Antarctica

AN Chunlei^{1, 2*}, WANG Yetang³ & HOU Shugui^{1, 4*}

¹ MOE Key Laboratory for Coast and Island Development, School of Geography and Oceanography, Nanjing University, Nanjing 210093, China;

² SOA Key Laboratory for Polar Science, Polar Research Institute of China, Shanghai 200136, China;

³ College of Geography and Environment, Shandong Normal University, Jinan 250014, China;

⁴ CAS Center for Excellence in Tibetan Plateau Earth Science, Beijing 100101, China

Received 10 December 2017; accepted 30 December 2017

Abstract Dome Argus (Dome A) in East Antarctica is a potentially likely site to meet one of the major objectives of the International Partnerships in Ice Core Sciences (IPICS) on the oldest ice core, and thus has aroused wide public and scientific interest. Since 2004/2005, many glaciological investigations have been conducted in this region. These have included GPS and ground-penetrating radar surveys, snow pit and ice core drilling, stake network measurements, and meteorological observations. In this article, the main results of these glaciological investigations in the Dome A region are summarized. We present details of the surface mass balance on different timescales and its spatial variability, geochemical characteristics of the surface snow, and paleo-environment reconstruction of ice cores. Finally, perspectives on the prospects for future studies are suggested.

Keywords Antarctic ice sheet, Dome A, glaciological observations, climate and environmental reconstruction

Citation: An C L, Wang Y T, Hou S G. Glaciological observations at Dome Argus, East Antarctica. *Adv Polar Sci*, 2017, 28 (4): 245-255, doi:10.13679/j.advps.2017.4.00245

1 Introduction

The Antarctic ice sheet (AIS) is one of the most important places in which to perform studies of climatic and environmental change. More than 90% of the Antarctic continent is covered by snow and ice, and any change in the vast ice sheet could affect sea level, the radiation budget (because of the high surface albedo of the AIS), and atmospheric and oceanic circulations. In addition to its participation in the present oceanic, atmospheric, and climatic systems, the AIS records information regarding past climatic and environmental changes. Currently, the longest two Antarctic ice core records are from Dome C and Dome F (also domes on the AIS), which cover the last 800,000 years (Jouzel et al., 2007) and 720,000 years

(Kawamura et al., 2017) respectively. However, it remains a considerable challenge to obtain ice core records extending back to the mid-Pleistocene (i.e., 1.5 Ma) to meet one of the major objectives of the International Partnerships in Ice Core Sciences (IPICS). Dome Argus (Dome A), the highest ice dome of the AIS, has the characteristics of particularly thick ice, extremely slow surface ice flow velocity, very low snow accumulation rates, and very low temperatures, which mean it is a location that could potentially provide valuable climatic information extending back to the mid-Pleistocene (Ren et al., 2009; Xiao et al., 2008). Because of this, it has aroused wide public and scientific interest. Additionally, Dome A is assumed an important source region for intensely cold air masses, which makes it suitable for observing climatic and environmental changes (Hou et al., 2007). However, because of the extremely harsh natural environment and relative inaccessibility of Dome A (far from the coast, high elevation and extremely low

* Corresponding authors: E-mail: An Chunlei, anchunlei@pric.org.cn; Hou Shugui, shugui@nju.edu.cn

temperature), almost no *in situ* surveys of this site had been made until the 21st Chinese National Antarctic Research Expedition (CHINARE) visited the summit of Dome A in the 2004/2005 austral summer, other than the third Soviet Antarctic Expedition traverse which passed about 80 km to the north of summit of Dome A in 1958 (Gan et al., 2016).

In preparation for future deep drilling projects, ground-based surface glaciological investigations were undertaken first by the 21st CHINARE in austral summer 2004/2005. These investigations included surface surveying and mapping, the installation of an automatic weather station (AWS), stake measurements, and snow pit and shallow ice core retrievals. In January 2009, China established the first research station (Kunlun Station, 80°25'01"S, 77°06'58"E, 4087 m a.s.l., about 7.3 km southwest to the summit of Dome A) in the Dome A region, which currently provides important support for regional scientific surveys. The ongoing deep ice core drilling project at Dome A, which commenced in 2010 (Li Y S et al., 2016; Zhang et al., 2014), had reached a drilling depth of 800 m by 2017.

This paper reviews the principal findings based on the results of surface glaciological observations acquired at Dome A since 2005. The main topics focus on the surface mass balance (SMB) and snow chemistry.

2 Study area

The summit of Dome A is located at 80°22'01.6"S, 77°22'22.9"E, approximately 1228 km from the coast and near the center of East Antarctica (Figure 1), and its elevation is 4092.5 m a.s.l. (Zhang et al., 2007, measured in January 2005). Actually, the surface near the summit is saddle-shaped and another peak exists to the south. The northern peak was ~ 30 cm (uncertainty: ~ 20 cm) lower than the southern peak in January 2008 (Cheng et al., 2009), but once again became ~ 7 cm higher (uncertainty: 3.5 cm) than the southern peak in January 2013 (Yang et al., 2014). This phenomenon might be caused mainly by uncertainty in measurements and in SMB variability. The results of GPS surveys during 2008–2013 indicate that, the surface velocity at 12 sites within an area of 1156 km² around Kunlun Station ranged from 3.1 ± 2.6 to 29.4 ± 1.2 cm·a⁻¹, with a mean value of 11.1 ± 2.4 cm·a⁻¹ (Yang et al., 2014). The surface flow directions tended to be nearly perpendicular to the surface elevation contours.

Based on ice radar investigations, the mean ice thickness in the Dome A central 30 × 30 km region is 2233 m, with a maximum ice thickness of 3139 m at Kunlun Station and a minimum ice thickness of 1618 m (Cui et al., 2010). Beneath the ice, there is a classic Alpine topography (Sun et al., 2009).

Based on the AWS measurements, the annual mean air temperature at 2 m above the surface (T_a) and firn temperature at 10 m depth (T_f) over the period 2005–2014

at Dome A were -52.1°C and -58.1°C respectively (Bian et al., 2016), while over the period 2005–2007 they were -51.6°C and -58.2°C respectively (Ma et al., 2010). The large difference between T_a and T_f is mainly caused by strong surface air-temperature inversions at Dome A.

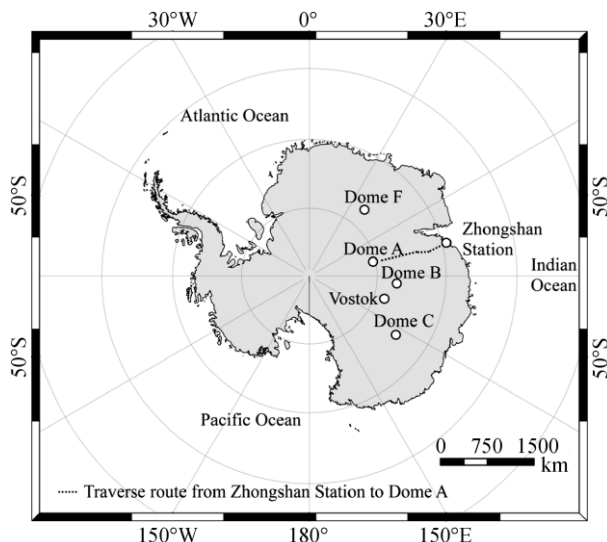


Figure 1 Location of Dome A in Antarctica.

3 Field observations

In January 2005, an AWS was installed at Dome A to measure various meteorological variables, which included air temperature, wind speed (both at heights of 1, 2, and 4 m above the snow surface), wind direction, atmospheric pressure, relative humidity, incoming solar radiation, surface snow height, and firn temperatures (at depths of 0.1, 1.0, 3.0, 5.0, and 10.0 m) (Xiao et al., 2007). A bamboo stake line (2-km spacing) and two stake arrays (a 5 × 5 matrix over a 100 × 100 m area, and a 7 × 7 matrix over a 30 × 30 km area) were installed to determine the SMB. The density of the surface snow at each site was measured to calculate the water equivalent accumulation. Unlike the bamboo stake method, the AWS provides hourly records of surface snow height, which can be used to explore both the seasonal variations and the effects of precipitation events and wind on SMB changes.

A dual-frequency radar system was used to detect the interior structure of the ice sheet over the Dome A region by the 21st CHINARE, these radar data have been used to reconstruct the spatial and temporal variability of SMB.

Surface snow, snow pit, and shallow ice core samples have been collected to investigate the chemical characteristics of depositions extending from the present to several thousand years in the past. Samples were sealed in clean bottles or bags and kept frozen during transportation from the field to the laboratory in China. The first ice core (DA2005 ice core), which was 109.9-m long, was retrieved in January 2005 at a location

approximately 300 m from the summit of Dome A. Subsequently, several shallow ice cores were recovered (the longest was 133 m, about 200 m from Kunlun Station). A deep ice core project at Kunlun Station commenced drilling in January 2012, aiming to reconstruct long-term variations of climate. 800-m of ice cores had been recovered by 2017. Continuous density measurements were made when collecting snow pit and ice core samples.

Field observations and sample collections have been performed principally during the CHINARE inland traverses from the coastal Zhongshan Station (Indian Ocean sector) to Dome A (Z-DA route) in the austral summers. As well as at Dome A, 7 AWS, 5 stake arrays and 1228-km of stake line (2-km spacing) for SMB measurements were established along the Z-DA route. GPS and ice radar investigations were carried out, and surface snow, snow pit, and shallow ice core samples were also collected. These provide the opportunity to compare the chemical parameters of surface snow between Dome A and other sites along the Z-DA route.

4 Results

4.1 SMB at Dome A

The SMB of the AIS is a key parameter to understanding the present state of the ice sheet, to estimating the contribution of ice sheet to sea level change, and to reconstructing the paleo climatic and environmental conditions. *In situ* measurements of SMB have been performed at Dome A by stakes, ultrasonic sounders, snow pits, ice cores, and ground-penetrating radar (GPR, also called ice-penetrating radar, snow radar, and sometimes radio echo sounding). These measurements provide valuable information on SMB local spatial variability and its temporal variability on different timescales (i.e., seasonal, annual, multi-decadal, centurial, and millennial). A summary of the main results based on these methods is presented in Table 1, together with some model results based on climate re-analysis datasets.

Table 1 Compilation of accumulation rates derived using different methods at Dome A

Period	Method	Accumulation rate/(kg·m ⁻² ·a ⁻¹)	References
1966–2005	Snow pit, β radioactivity peak	23	Hou et al. 2007
1965–2009	Snow pit, β radioactivity peak	21	Wang et al. 2013
1260–1964	Ice core, volcanic stratigraphic markers	23.2	Jiang et al., 2012
2008–2013	Stake array, 30 × 30 km	22.9 ± 5.9	Ding et al. 2016
Last 47.5 ka	Radio-echo sounding	22.1	Wang et al. 2016
Last 161 ka	Radio-echo sounding	17.2	Wang et al. 2016
1980–2002	Climate re-analysis, ERA-40	10	Wang et al. 2013
1979–2012	Climate re-analysis, ERA-interim	8	Ding et al. 2016
1979–2012	Climate re-analysis, MERRA	13	Ding et al. 2016
1979–2012	Climate re-analysis, JRA-55	21	Ding et al. 2016

Many factors could influence the uncertainty of SMB derived from the above measurements (Eisen et al., 2008). Before the discussion of the characteristic of SMB, we must consider the uncertainties, representativeness, and limitations of the methods. The main error sources for the various methods are summarized in Table 2. In general, in regions with a low accumulation rate, single stakes or cores are not representative on an annual scale, and only long-term observations will result in reliable accumulation values. Stake or ultrasonic measurements are the only way to detect zero accumulation or erosion values on an annual or seasonal scale. SMB based on GPR and stake lines could show the representativity of spot measurements (in general, only representative within a small area of a few square kilometers around the site) (Eisen et al., 2008). The characteristic and uncertainties of these measurements at Dome A are summarized as follows:

(1) Stakes

With consideration of density measurements, height

measurements, and the densification process, the calculated SMB uncertainty is within 2% (Ding et al., 2016), while total error is <4.6% for the Z-DA route (but not spatially constant) (Ding et al., 2015).

Table 2 Main error sources of SMB estimates for different methods

Error sources	Methods	Stakes	Ultrasonic sounders	Snow pits	Ice cores	GPR
Submergence		●	●			
Disturbance of the snow surface		●	●			
Density measurement		●	●	●	●	●
Length/depth measurement		●	●	●	●	●
Age dating				●	●	●
Dynamic layer thinning					●	●
Flow of ice					●	●

(2) Ultrasonic sounders

The Campbell Scientific SR50-45 ultrasonic distance sensor, which is widely used in Antarctica, is mounted on the 4 m arm of the AWS. The measurement accuracy is ± 1 cm or 0.4% of the distance to the surface (Ma et al., 2010; Xiao et al., 2008).

(3) Snow pits

The 1964/1965 β -radioactive marker was utilized to determine the average accumulation rate (Wang et al., 2013; Hou et al., 2007). The typical error for snow pits is less than 10% (Eisen et al., 2008).

(4) Ice cores

Two volcanic stratigraphic markers, corresponding to the 1963 Agung and an unknown 1259 eruptions, are used to date the DA2005 ice core and calculate the SMB. The error of age determination due to thinning is about 10 a at the bottom of the core (109.9 m, 3186 a BP (present = end of AD 1998)) (Jiang et al., 2012).

(5) GPR

A model is used to estimate the effects of spatial gradients in accumulation rates because of the ice flow by Wang et al. (2016). Their result suggests that even the deepest and oldest layers studied are not significantly affected by spatial variability in accumulation. Uncertainties caused by other factors are mostly due to the age dating (personal communication with the author). The dating error is discussed in section 4.1.1.

4.1.1 Temporal variability

On the seasonal scale, continuous surface snow height measurements by ultrasonic sounders provide valuable data to investigate accumulation patterns at Dome A. Measurements during 2005–2007 reveal that there was little change in snow surface height between January and April, then large fluctuations occurred between May and mid-October (but suspected to be due to a problem with the sensor operation in the extremely low winter temperatures), and the major accumulation period was between October and December (Ma et al., 2010; Xiao et al., 2008). This seasonality of snow accumulation at Dome A appears different to that at Vostok (maximum in winter), Dome F (no seasonal cycle), and in Dronning Maud Land (large interannual variability), all also on the East Antarctic Plateau (Wang et al., 2013). However, because of the short observation period, it needs to be confirmed by longer time records.

There is considerable annual variability in SMB at Dome A. The surface snow height change derived from ultrasonic sounders was 11, 5, and 19 cm in 2005, 2006, and 2007, respectively (Ma et al., 2010). Negative values have also been recorded in some years from the single stake measurements (Ding et al., 2015). Measurements of the 100×100 m stake array provide the opportunity to assess the representativity of single stake/spot measurements. These

data show that there are still large spatial variations in the mean SMB over periods of 2–3 a (2005–2013), but the magnitude of the variation decreases over longer timescales. The relative standard deviation of SMB decreases from 81% to 19% when the observation time span increases from 2 a (2011–13) to 5 a (2008–2013) (Ding et al., 2016, 2015). Large inter-annual fluctuations might reflect not just the variation of precipitation, but also the effects of local noise on single stake measurements. Short-term signals might be missed when using snow pit and/or ice core samples from Dome A; therefore, records on multiyear or longer temporal scales are more reliable for paleo-reconstruction.

Based on snow pit samples at Dome A, the mean accumulation rate during 1966–2005 was $23 \text{ kg}\cdot\text{m}^{-2}\cdot\text{a}^{-1}$ (Hou et al., 2007). Another snow pit (located at Kunlun Station) produced a result of $21 \text{ kg}\cdot\text{m}^{-2}\cdot\text{a}^{-1}$ between 1965 and 2009 (Wang et al., 2013). The results of these two studies are quite close to each other, indicating the reliability of these values for the reconstruction of mean SMB over the past few decades. Overall, the value of SMB at Dome A is lower than or comparable to that at Dome F ($28.8 \pm 0.7 \text{ kg}\cdot\text{m}^{-2}\cdot\text{a}^{-1}$ during 1964–2008, Fujita et al., 2011), Dome C ($26\text{--}33 \text{ kg}\cdot\text{m}^{-2}\cdot\text{a}^{-1}$ during 1966–1998, Frezzotti et al., 2004), and Vostok ($22.9 \pm 1.8 \text{ kg}\cdot\text{m}^{-2}\cdot\text{a}^{-1}$ during 1970–1995, Ekaykin et al. 2004).

Using two known volcanic stratigraphic markers in an ice core recovered from Dome A, the mean SMB during 1260–1964 has been estimated as $23.2 \text{ kg}\cdot\text{m}^{-2}\cdot\text{a}^{-1}$ (Jiang et al., 2012). Wang et al. (2013) have re-assessed the SMB between 1260 and 2005 and produced values of $22\text{--}25 \text{ kg}\cdot\text{m}^{-2}\cdot\text{a}^{-1}$. These results reveal that the accumulation rate at Dome A has been extremely low and that it appears to have been stable on multi-decadal/centennial scales over the past 700 years.

Radio-echo sounding (RES) measurements reveal the pattern of SMB on millennial or longer timescales by tracing isochronous internal layering within the ice sheet. By linking six layers at Dome A with an ice core from Vostok, estimates of the SMB for the past ~ 161 ka have been derived (Wang et al., 2016). The SMB of the past 34 ka was found comparable in terms of magnitude with that derived from snow pit and ice core samples; however, a relatively higher value of the SMB was found for the period 34–47 ka BP (i.e., Marine Isotope Stage 3) (Figure 2).

4.1.2 Spatial variability

GPR measurements show that the SMB slightly increases from south to north along the 216 km radar profile at Dome A for the past ~ 161 ka; part of this profile is shown in Figure 2. Although the SMB over different time periods (refer to the time periods (TP) in Figure 2) show considerable difference, the spacial variation within a period is quite small, especially for the past 34 ka. Another notable feature is that, compared to the south of Dome A, larger variations of SMB appear in the north.

Multiyear stake network observations could also

present a general picture of the spatial variability of the SMB. Measurements of the 30×30 km stake array show that there was no significant spatial variation in the mean SMB, averaged from 2008 to 2013, except for a few slightly

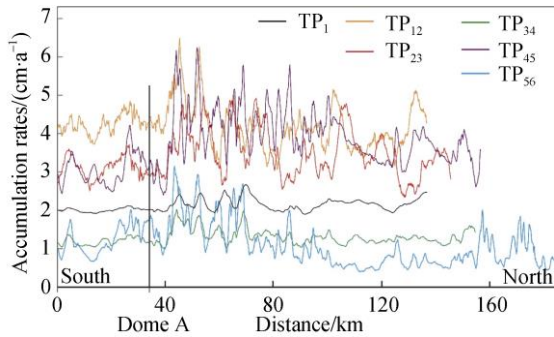


Figure 2 Accumulation rates for the past ~161 ka derived from RES data. Calculated accumulation rates (in ice equivalent, $\rho = 917 \text{ kg}\cdot\text{m}^{-3}$) averaged for different time periods along the RES profile. The location of Dome A is shown by the black vertical line (34 km from the origin). TP1: $0\text{--}34.3 \pm 1.3$ ka BP; TP12: $34.3 \pm 1.3\text{--}39.6 \pm 0.1$ ka BP; TP23: $39.6 \pm 0.1\text{--}47.5 \pm 1.7$ ka BP; TP34: $47.5 \pm 1.7\text{--}93.3 \pm 0.4$ ka BP; TP45: $93.3 \pm 0.4\text{--}123.5 \pm 1.5$ ka BP; TP56: $123.5 \pm 1.5\text{--}161.4 \pm 1.0$ ka BP (adapted from Wang et al., 2016).

high values in western parts (Figure 3) (Ding et al., 2016). Mean accumulation rate of the whole region during 2008–2013 was $22.9 \pm 5.9 \text{ kg}\cdot\text{m}^{-2}\cdot\text{a}^{-1}$ (Ding et al., 2016), very close to the results derived from snow pits and ice core samples.

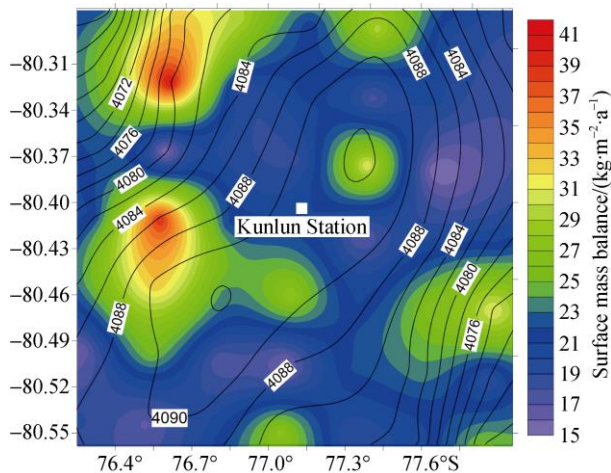


Figure 3 Map of the mean (2008–2013) SMB across Dome A. Elevation contours (m) are also shown (adapted from Ding et al., 2016).

4.1.3 Factors influencing SMB variability

SMB of the AIS could be influenced by many factors, such as precipitation, surface sublimation, wind-driven snow redistribution (erosion/deposition), and local topography.

The homogeneity of precipitation can be reduced near ridges and domes, which might lead to slight spatial variations in SMB (Genthon et al., 2016). Across Dome A, clear-sky precipitation and frost comprise a large fraction of the total precipitation (Hou et al., 2007), resulting in a very special needle-shaped or feather-shaped ice crystal layer at the surface which is easily affected by wind. However, based on AWS measurements during 2005–2011, the wind speed in most months appears to be $< 3 \text{ m}\cdot\text{s}^{-1}$ without any prevailing direction; thus, the impact of wind-driven processes on SMB might be small. Probably due to the gentle local topography and the lack of a dominant wind direction, no significant correlation is found between SMB and topographic variables such as elevation, slope gradient, and aspect (Wang et al., 2013). Despite extremely low wind speed and air temperature, the surface sublimation has a considerable negative contribution to the SMB, about $-0.85 \pm 0.02 \text{ mm w.e.}\cdot\text{a}^{-1}$ (Ding et al., 2016). The above factors might help understand the characteristic of SMB around Dome A.

4.2 Snow chemistry

The chemical parameters of snow/ice on the polar ice sheet, including the isotopic composition of the snow and the chemical characteristics of impurities in the snow, could be used to reconstruct the history of climate change, atmospheric circulation, and impact of anthropogenic activities (Kreutz and Mayewski, 1999; Legrand and Mayewski, 1997).

4.2.1 Stable isotopes of snow/ice

Stable isotopic composition (δD , $\delta^{18}\text{O}$, and $\delta^{17}\text{O}$) of snow/ice on the AIS is among the most valuable proxies in climate studies (Hou et al., 2013).

Both δD and $\delta^{18}\text{O}$ are correlated strongly with local temperature and thus, they are used widely for paleo-temperature reconstruction. The values of δD and $\delta^{18}\text{O}$ in the ice cores from Vostok and EPICA Dome C reflect the glacial–interglacial climatic cycles over the past 400 and 800 ka, respectively (Jouzel et al., 2007; Petit et al., 1999). Averaged $\delta^{18}\text{O}$ and δD values of the DA2005 ice core were determined as -58.5‰ and -450.6‰ , respectively (Hou et al., 2009). These are lower than derived from surface snow (depth: 3–5 cm) collected during summer: averaged $\delta^{18}\text{O}$ and δD values of -54.5‰ and -411.3‰ respectively for the upper 5 cm of snow (Xiao et al., 2013), and -52.3‰ and -402.1‰ respectively for the upper 3 cm of snow (Ma et al., 2017). Based on the mean annual accumulation rate at Dome A, the difference between surface snow and ice core records might partly reflect that the deposition from winter are not fully involved in the 3–5 cm surface snow samples. Compared with other interior AIS sites at high elevation over similar depositional periods (e.g., Dome B, Dome C, Dome F, and Vostok), the averaged $\delta^{18}\text{O}$ and δD values of the DA2005 ice core and

snow pit samples are the lowest (Hou et al., 2009; Xiao et al., 2007).

To reconstruct paleo-temperature variability based on ice core records, quantification of the spatial and temporal relationships between δ and T is a prerequisite. Unfortunately, there are usually too few long-term observations with which to construct a reliable temporal function at a single site in the interior of the AIS. Thus, for AIS ice core interpretation, most studies have used the spatial δ - T function based on surface snow data (Hou et al., 2013; Goosse et al., 2012; Schneider and Noone, 2007). However, the spatial δ - T slopes vary regionally (Wang et al., 2009; Masson-Delmotte et al., 2008). For the entire continent, the spatial slopes are $0.80\text{‰}\cdot\text{°C}^{-1}$ for $\delta^{18}\text{O}$ - T and $6.34\text{‰}\cdot\text{°C}^{-1}$ for δD - T (Masson-Delmotte et al., 2008). For the Z-DA route, the corresponding values are $0.84\text{‰}\cdot\text{°C}^{-1}$ for $\delta^{18}\text{O}$ - T (Ding et al., 2010) and $6.5\text{‰}\cdot\text{°C}^{-1}$ for δD - T (Xiao et al., 2013). For the region around Dome A, the value for $\delta^{18}\text{O}$ - T is $0.94\text{‰}\cdot\text{°C}^{-1}$ (Pang et al., 2015). Based on the evolution of δD from the DA2005 ice core, the climate at Dome A has been reasonably stable during the late Holocene (Hou et al., 2009).

The d -excess, defined as $\delta\text{D}-8\delta^{18}\text{O}$, reflects kinetic fractionation processes. It is controlled primarily by the condensation temperature at the precipitation site and the conditions at the moisture source region (including sea surface temperature, relative humidity, and wind speed). It is usually used as an indicator of moisture source (Hou et al., 2013; Vimeux et al., 2001; Jouzel and Merlivat, 1984; Merlivat and Jouzel, 1979). The d -excess values of surface snow and shallow ice core samples at Dome A have been calculated as 24.6‰ (Xiao et al., 2013) and 17.1‰ (Hou et al., 2009), respectively. The values at Dome A are higher than at the coast (12.4‰) and at elevations below 2750 m along the Z-DA route (11.6‰) (Xiao et al., 2013). The DA2005 ice core shows a decreasing trend of the value of d -excess since the late Holocene (Hou et al., 2009). The sensitivity of d -excess at Dome A to the temperature and relative humidity at the moisture source region and to the local temperature has been quantified using the Mixed Cloud Isotopic Model based on d -excess datasets acquired along the Z-DA route: $\Delta d\text{-excess} = 1.6\Delta T_{\text{source}} - 1.8\Delta T_{\text{site}} - 0.18\Delta RH$ (Pang et al., 2015). Because the local temperature and the conditions at the moisture source region were relatively stable during this period, this trend probably reflects the migration of the source region of the precipitation toward lower latitudes (Hou et al., 2009).

The ^{17}O -excess is defined as $10^6 \times (\ln(\delta^{17}\text{O}/1000 + 1) - 0.528\ln(\delta^{18}\text{O}/1000 + 1))$. Different to the d -excess, the ^{17}O -excess is controlled mainly by the relative humidity at the moisture source region, and it is not sensitive to the source temperature and water $\delta^{18}\text{O}$ in oceanic regions (Risi et al., 2010; Uemura et al., 2010; Landais et al., 2008; Angert et al., 2004). Therefore, the combination of d -excess and ^{17}O -excess could be useful for furthering understanding of stable isotopic kinetic fractionation processes. However,

many factors could affect the ^{17}O -excess of precipitation in polar region (Pang et al., 2015). Currently, available data are sparse because high-precision measurements of $\delta^{17}\text{O}$ in water were unavailable before 2005 (Barkan and Luz, 2005). Therefore, the processes controlling ^{17}O -excess in polar regions are still not understood fully.

Pang et al. (2015) reported that the value of ^{17}O -excess in the surface snow over the Dome A region (21 per meg) is lower than at the coast and other low-elevation regions along the Z-DA route. This might be because of the influence of the supersaturation effect on ^{17}O -excess at low temperatures (Pang et al., 2015). However, there is no significant correlation between ^{17}O -excess values and condensation temperature at the cold interior deep-ice-core drilling sites over the AIS (i.e., Dome A, Dome C, Vostok, and Dome F). Furthermore, very high and low ^{17}O -excess values can be found at both interior and coastal regions across the entire AIS. This suggests the spatial distribution of ^{17}O -excess on the AIS cannot be explained only by the condensation temperature or by the moisture source location and its relative humidity (Pang et al., 2015).

4.2.2 Impurities in the snow/ice

Here, we present a summary and analysis of the observations of impurities found in the snow/ice at Dome A, including Na^+ , Cl^- , Mg^{2+} , SO_4^{2-} , methanesulfonic acid (MSA), nitrate (NO_3^-), arsenic (As), mercury (Hg), formate, acetate, bacteria, and CH_4 .

(1) Na^+ , Cl^- , and Mg^{2+}

Na^+ , Cl^- , and Mg^{2+} in the snow/ice on the AIS are derived primarily from sea salt (Legrand and Mayewski, 1997); thus, they are referred to usually as “sea salt ions”. These ions generally peak in winter because of increased storm intensity and/or frequency (Kreutz and Mayewski, 1999). Over Dome A and the Z-DA route, these three ions in the samples obtained from both the surface and the snow pits are highly positively correlated with each other (Li C et al., 2016), implying they originate from the same source. Similar to studies in other regions, the mean concentrations of these ions in the snow pits at Dome A (i.e., the interior) are lower than at coastal regions; however, a seasonal cycle could not be determined at Dome A because of the low accumulation rate.

(2) SO_4^{2-} and MSA

SO_4^{2-} is another major ion in the snow/ice on the AIS. It originates mainly from non-sea-salt (nss) sources. The majority of nssSO_4^{2-} is derived from the oxidation of dimethylsulfide (DMS) produced by marine biota (Legrand and Mayewski, 1997). In addition, volcanic emissions also contribute to the nssSO_4^{2-} , with sporadic and short-term inputs. Because of this, nssSO_4^{2-} is used widely to reconstruct the history of volcanism and to date ice cores. MSA is derived only from the oxidation of DMS. The annual cycles of MSA and nssSO_4^{2-} usually peak in summer, corresponding to the period of maximum biologic

productivity (Kreutz and Mayewski, 1999).

Unlike sea salt ions, no clear trend has been established when comparing the mean concentrations of MSA and nssSO_4^{2-} found in snow pits at Dome A with those at the coast or at other sites along the Z-DA route (Li C et al., 2016). The MSA fraction ratio, defined as $\text{MSA}/(\text{MSA} + \text{nssSO}_4^{2-})$, could be used to diagnose the moisture source because marine air masses from lower latitudes are characterized by lower MSA/ nssSO_4^{2-} ratios (attributable to the higher temperatures at the source areas) (Becagli, 2004; Legrand and Pasteur, 1998). The mean MSA fraction ratio measured at Dome A is 0.10 (W/W), markedly lower than at coastal sites (0.23 ± 0.01 (W/W)). This might reflect a greater fraction of air masses from lower latitudes at Dome A than at coastal sites (Li C et al., 2016).

High SO_4^{2-} concentrations from volcanic eruptions at known dates are important signals for dating ice cores. Volcanic event markers shown by prominent values of nssSO_4^{2-} have been used to date the DA2005 ice core (Figure 4). Jiang et al. (2012) used two recognizable volcanic stratigraphic markers (1963 Agung (Indonesia) and 1259 unknown eruptions) to compute the mean accumulation rate. Then, they used the result of $23.2 \text{ mm w.e.}\cdot\text{a}^{-1}$ to date the entire core. They found good agreement between the years of the expected appearances and the calculated ages of all the well-dated volcanic events of the last two millennia. The age at the bottom of this core (depth: 109.91 m) is 3186 a BP (present = end of AD 1998) (Jiang et al., 2012). Differently from Jiang et al. (2012), Li et al. (2012) used the Pinatubo eruption in 1050 BC as a reference layer with which to determine the age of the bottom of this core, which produced a date of 4009 ± 150 a BP. However, they also highlighted that no previous studies had mentioned the Pinatubo signal in polar ice cores, and that the dating inaccuracy for the Pinatubo event could cause age dating discrepancy. In future, better-dated volcanic records in Antarctic ice cores, ideally from sites with high accumulation rates, should be used to corroborate the DA2005 core.

Ice cores from the polar regions perhaps provide the best means with which to evaluate the impact of past volcanism on the global climate. A detailed history of volcanism has been reconstructed from the top 100.42 m of the DA2005 ice core by detecting outstanding sulfate events. Based on the results of a study by Jiang et al. (2012), which covered the period from 840 BC to AD 1998, 78 eruptions have been identified. From AD 1000 to 1998, the DA2005 record shows good agreement with previous records. From AD 1–1000, the record also presents a series of volcanic signatures that could be found in both the DA2005 record and several other Antarctic ice core records. However, for older periods, direct comparison between the DA2005 record and other Antarctic ice core records is difficult because of the lack of well-dated stratigraphic horizons.

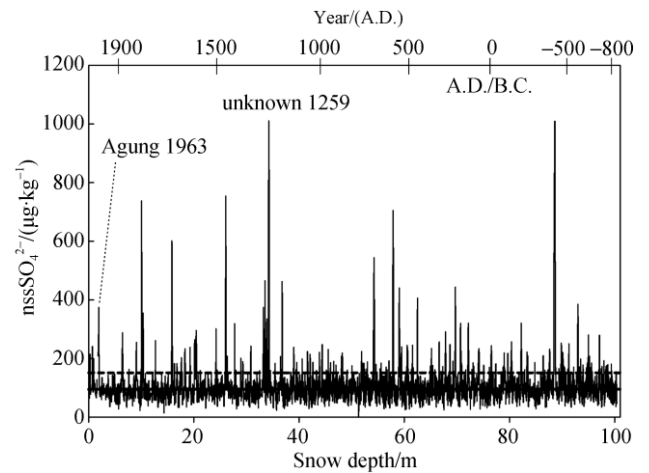


Figure 4 Continuous profile of nssSO_4^{2-} concentrations in the DA2005 ice core as a function of snow depth. Solid horizontal line indicates the non-volcanic background, and the dashed horizontal line represents the detection threshold (background $\pm 2\sigma$) (adapted from Jiang et al., 2012).

(3) NO_3^-

NO_3^- is also among the major ions found in the snow/ice on the AIS. Various sources of nitrogen oxides (NO_x) can contribute to the NO_3^- budget of polar precipitation, e.g., soil microbial activity, biomass burning, fossil fuel combustion, lightning, galactic cosmic rays, stratospheric oxidation of N_2O , and ionospheric dissociation of N_2 (Delmas et al., 1997; Legrand and Kirchner, 1988). The high number of input sources and complex post-depositional processes (e.g., photolysis and possible volatilization as HNO_3) make it very difficult to assess the primary sources of nitrate and their paleo-environmental significance (Wolff, 1995). Measurements of the nitrogen and oxygen stable isotope ratios in NO_3^- have provided constraints for past NO_x sources and oxidation chemistry (Hastings, 2010; Hastings et al., 2009; Alexander et al., 2004). In the atmosphere, the oxygen isotopes in NO_3^- reflect oxidants involved in the production of NO_3^- , whereas the nitrogen isotopes can reflect NO_x sources and the possible imprints of transport and chemistry.

Shi et al. (2014) studied mass fraction and isotopic composition ($\delta^{15}\text{N}$ and $\delta^{18}\text{O}$) of NO_3^- in a 3-m snow pit at the summit of Dome A (Figure 5). In their study, the highest snow NO_3^- mass fractions (hereafter, $w(\text{NO}_3^-)$) were found in surface snow. However, they fell sharply with depth from $> 200 \text{ ng}\cdot\text{g}^{-1}$ to below $20 \text{ ng}\cdot\text{g}^{-1}$ within the top 30 cm. This finding is similar to Dome C, where $w(\text{NO}_3^-)$ was found to decrease from hundreds of nanograms per gram in the surface snow to only tens of nanograms per gram at a depth of 10 cm (Röthlisberger et al., 2000). The marked trend of decrease of $w(\text{NO}_3^-)$ with depth seems to fit an exponential model. The $\delta^{15}\text{N}$ of nitrate is lower in the surface layers and it increases rapidly with depth in the upper 30 cm, while the $\delta^{18}\text{O}$ of nitrate shows the opposite trend. The trend of decrease of $\delta^{18}\text{O}$ (NO_3^-) with increasing

$\delta^{15}\text{N}$ (NO_3^-) indicates secondary formation of nitrate *in situ* (following photolysis) with a low $\delta^{18}\text{O}$ source. Below 30 cm, the $\delta^{18}\text{O}$ (NO_3^-) was found to increase gradually toward the bottom of the pit. A significant negative relationship has

been established between $w(\text{NO}_3^-)$ and $\delta^{18}\text{O}$ (NO_3^-) at depths of 100–200 cm, which reflects the complexity of the post-depositional processing of nitrate and the sensitivity of the nitrate isotopic composition to this processing.

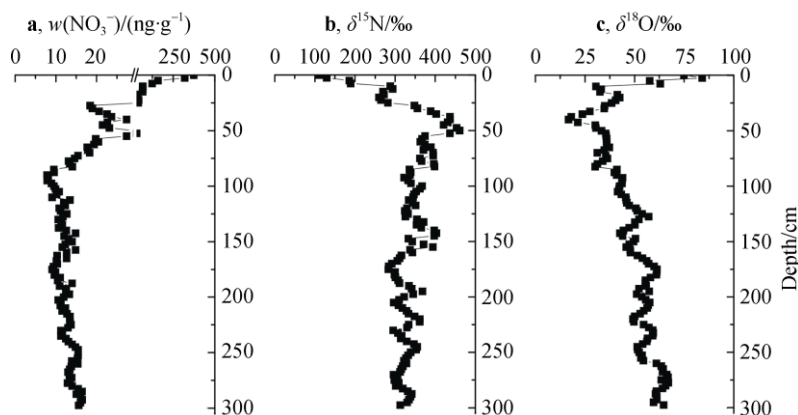


Figure 5 Detailed profiles of $w(\text{NO}_3^-)$ (a) and isotopic composition $\delta^{15}\text{N}$ (b) and $\delta^{18}\text{O}$ of NO_3^- (c) in the snow pits at Dome A. Note that the x-axis of $w(\text{NO}_3^-)$ is broken to display the trend in deeper snow (adapted from Shi et al., 2014).

(4) Arsenic

Arsenic is a highly toxic element that poses great danger to human health. The Antarctic ice sheet is an ideal site for studying historical trace metal deposition. At Dome A, studies have shown that arsenic deposited in the snow during 1964–2009 is most probably from anthropogenic emissions, not natural contributors (Hua et al., 2016). Arsenic concentrations found at Dome A range from approximately 0.5 to 25.0 $\text{pg}\cdot\text{g}^{-1}$ with a mean concentration of 4.7 $\text{pg}\cdot\text{g}^{-1}$. The values increased substantially from the mid-1980s to the late 1990s, before decreasing during the late 1990s and remaining at low levels until 2009. This pattern might reflect the increase in copper smelting in South America (for the increasing trend) and subsequent environmental regulation (for the decreasing trend). Combining the results of arsenic studies at Dome F and arsenic levels found in Antarctica Ice Core-6 (81°03' S, 79°50' E), Hua et al. (2016) concluded that arsenic pollution from the mid-1980s to the late 1990s in Antarctica was a regional phenomenon, and that South America was the primary source region for that part of Antarctica facing the Atlantic and Indian oceans.

(5) Mercury

Mercury (Hg) is a trace metal pollutant of global concern because of its relatively long atmospheric residence time (approximately 1 a) and its potential to form highly toxic methylmercury, which can bioaccumulate in the aquatic food chain. Determining the spatial and temporal patterns of atmospheric mercury deposition is important because the atmosphere is the main pathway for the dispersion of this toxic metal (Boutron et al., 1998; Fitzgerald and Clarkson, 1991).

Total Hg (THg) concentrations in the surface snow at Dome A have been found to be much higher than at sites near the coast (Li et al., 2014). This spatial distribution

pattern is very similar to that between Syowa Station and Dome F (Han et al., 2011). THg concentrations in surface snow are much higher than the mean concentrations in snow pits, reflecting post-depositional loss effects. However, unlike the distribution pattern in surface snow, there is little difference between the mean concentrations in the snow pits at Dome A and at coastal sites, despite the annual net deposition rate in the snow pits at Dome A being lower than at the coastal sites. High THg concentrations appeared at the end of the 1970s and during the 1980s, which could be related to increased amounts of global Hg production and associated anthropogenic emissions. Elevated levels of THg concentration, which occurred in the early 1990s, could have been caused by the Mount Pinatubo eruption (1991).

(6) Formate and acetate

Carboxylic acids in polar ice appear useful for investigating the history of biomass burning and past vegetation emissions (Legrand and Mayewski, 1997). Vegetation emissions influence the background level of carboxylic acids present in polar precipitation over the preindustrial era, and forest fires influence the short-term variations. Formate and acetate are the chief carboxylic compounds present in the troposphere. Talbot et al. (1988) found that anthropogenic emissions (i.e., motor vehicles and biomass combustion) are important sources of atmospheric acetic acid and that these sources have formic-to-acetic ratios much less than 1.0, while natural sources (vegetation emissions in particular) had ratios larger than one.

At Dome A, the mean concentrations of formate and acetate in a 3-m-deep (1973–2012) snow pit were found to be 1.13 ± 0.40 and 6.46 ± 2.01 $\text{ng}\cdot\text{g}^{-1}$, respectively (Li et al., 2015), i.e., lower than surface snow samples in summer. Both monocarboxylic acids displayed a significant trend of increase in the 1970s. In the 1980s, they exhibited a sudden

reduction initially, followed by an increase. In the 1990s, the trend was of slight decrease until 2004, following which it increased markedly to 2012. The increases in the concentrations of monocarboxylic acids since 2005 were temporally coincident with Chinese expedition activities in the area. The mean formate-to-acetate ratio was found to be 0.18 ± 0.05 , i.e., much lower than one. These findings suggest that local anthropogenic activities might be responsible for the increases in the acid load during recent decades.

Spatially, the deposition rates and mean concentrations of the two acids in inland snow pits (600–1248 km from the coast) were found lower than at coastal areas (0–600 km from the coast), particularly with regard to formate (Li et al., 2015).

(7) Bacteria

Yan et al. (2012) studied the concentrations of cultured bacteria in a 1.6-m snow core at Dome A and in three other cores obtained along the Z-DA route. At Dome A, they found the average concentration of cultured bacteria isolated from the snow core was $0.008 \text{ CFU} \cdot \text{mL}^{-1}$. Members of *Alphaproteobacteria* were found in this core, and isolates of the *Brevundimonas* genus were recovered, although there was only one strain. Spatially, along the Z-DA route, the abundance and diversity of cultured bacteria decreased with increasing latitude, elevation, and distance from the coast. Furthermore, concentrations of cultured bacteria along the route were found lower than in ice cores taken from mountain glaciers.

(8) CH₄

CH₄ measurements have been undertaken to determine the close-off depth (where bubble air is occluded completely) of the DA2005 ice core (Hou et al., 2009). The CH₄ concentrations, above the depth of 102.0 m, were >1400 ppbv, which is equivalent to atmospheric CH₄ concentrations since the Industrial Revolution. Below this depth, CH₄ concentrations were found to decrease gradually to atmospheric values prior to the Industrial Revolution. This clear transition indicates a close-off depth at about 102.0 m at Dome A under present climate conditions.

5 Summary and outlook

Surface glaciological observations obtained at Dome A since 2004/2005 have helped elucidate the state and mechanism of environmental change in this highest region of the AIS. Surface topography and velocity observations have revealed a largely flat surface and a very slow ice surface velocity. SMB studies have revealed relative stability on multiyear or longer timescales, although annual and seasonal fluctuations are large. Geochemical analysis has provided a link between the surface snow/ice and the site temperature, moisture source, atmospheric impact of anthropogenic activities, atmospheric circulation, and post-depositional process. In addition, the ice core records have helped establish the history of past climate change and volcanism.

We suggest the following issues should be addressed in the future:

(1) Research on long-sequence climate records. The extremely low accumulation rate and ice flow velocity make Dome A an ideal region for long-term studies of the climatic record; however, research results in this subject area remain scant.

(2) Research on modern processes of snow accumulation. To investigate the accumulation pattern, the air–snow relationships in relation to chemical parameters as well as the relationships between instrumental records and climate/environmental proxy records will help improve understanding of the regional climate and the quality of the calibration/verification of the reconstructions.

(3) Combinations of observations and model simulations might help clarify the mechanism and impact of climatic and environmental change at Dome A.

Acknowledgments This work was supported by the Natural Science Foundation of China (Grant no. 41330526), Natural Science Foundation of Shanghai (Grant no. 17ZR1433200), and National Key R & D Program of China (Grant no. 2016YFC1400302). Our thanks go to Jiang Su, Ding Minghu, Ma Tianming, and Wang Tiantian for their help with the figures, to Ling Xiaoliang and Shi Guitao for their useful suggestions, to the CHINARE for support regarding the field observations at Dome A, and to the editor and reviewers for their constructive comments.

References

- Alexander B, Savarino J, Kreutz K J, et al. 2004. Impact of preindustrial biomass-burning emissions on the oxidation pathways of tropospheric sulfur and nitrogen. *J Geophys Res*, 109(D8): D08303, doi: 10.1029/2003JD004218
- Angert A, Cappa C D, DePaolo D J. 2004. Kinetic ¹⁷O effects in the hydrologic cycle: Indirect evidence and implications. *Geochim Cosmochim Acta*, 68(17): 3487–3495, doi: 10.1016/j.gca.2004.02.010
- Barkan E, Luz B. 2005. High precision measurements of ¹⁷O/¹⁶O and ¹⁸O/¹⁶O ratios in H₂O. *Rapid Commun Mass Spectrom*, 19(24): 3737–3742, doi: 10.1002/rcm.2250
- Becagli S, Benassai S, Castellano E, et al. 2004. Chemical characterization of the last 250 years of snow deposition at Talos Dome (East Antarctica). *Int J Environ Anal Chem*, 84(6–7): 523–536, doi: 10.1080/03067310310001640384
- Bian L G, Allison I, Xiao C D, et al. 2016. Climate and meteorological processes of the East Antarctic ice sheet between Zhongshan and Dome-A. *Adv Polar Sci*, 27(2): 90–101, doi: 10.13679/j.advps.2016.2.00090
- Boutron C F, Vandal G M, Fitzgerald W F, et al. 1998. A forty year record of Mercury in central Greenland snow. *Geophys Res Lett*, 25(17): 3315–3318, doi: 10.1029/98GL02422
- Cheng X, Gong P, Zhang Y M, et al. 2009. Surface topography of Dome A, Antarctica, from differential GPS measurements. *Journal of Glaciology*, 55(189): 185–187, doi: 10.3189/002214309788608868
- Cui X B, Sun B, Tian G, et al. 2010. Ice radar investigation at Dome A, East Antarctica: Ice thickness and subglacial topography. *Chin Sci*

- Bull, 55(4–5): 425–431, doi: 10.1007/s11434-009-0546-z
- Delmas R, Serça D, Lambert C. 1997. Global inventory of NO_x sources. *Nutr Cycl Agroecosys*, 48(1–2): 51–60, doi: 10.1023/A:1009793806086
- Ding M H, Xiao C D, Jin B, et al. 2010. Distribution of δ¹⁸O in surface snow along a transect from Zhongshan Station to Dome A, East Antarctica. *Chin Sci Bull*, 55(24): 2709–2714, doi: 10.1007/s11434-010-3179-3
- Ding M H, Xiao C D, Li C J, et al. 2015. Surface mass balance and its climate significance from the coast to Dome A, East Antarctica. *Sci China Earth Sci*, 58(10): 1787–1797, doi: 10.1007/s11430-015-5083-9
- Ding M, Xiao C, Yang Y, et al. 2016. Re-assessment of recent (2008–2013) surface mass balance over Dome Argus, Antarctica. *Polar Res*, 35(1): 26133, doi: 10.3402/polar.v35.26133
- Eisen O, Frezzotti M, Genthon C, et al. 2008. Ground-based measurements of spatial and temporal variability of snow accumulation in East Antarctica. *Rev Geophys*, 46(2): RG2001, doi: 10.1029/2006RG000218
- Ekaykin A A, Lipenkov V Y, Kuzmina I N, et al. 2004. The changes in isotope composition and accumulation of snow at Vostok station, East Antarctica, over the past 200 years. *Ann Glaciol*, 39: 569–575, doi: 10.3189/172756404781814348
- Fitzgerald W F, Clarkson T W. 1991. Mercury and monomethylmercury: present and future concerns. *Environ Health Perspect*, 96: 159–166
- Frezzotti M, Pourchet M, Flora O, et al. 2004. New estimations of precipitation and surface sublimation in East Antarctica from snow accumulation measurements. *Climate Dyn*, 23(7–8): 803–813, doi: 10.1007/s00382-004-0462-5
- Fujita S, Holmlund P, Andersson I, et al. 2011. Spatial and temporal variability of snow accumulation rate on the East Antarctic ice divide between Dome Fuji and EPICA DML. *Cryosphere*, 5(4): 1057–1081, doi: 10.5194/tc-5-1057-2011
- Gan I, Drewry D, Allison I, et al. 2016. Science and exploration in the high interior of East Antarctica in the twentieth century. *Adv Polar Sci*, 27(2): 65–77, doi: 10.13679/j.advps.2016.2.00065
- Genthon C, Six D, Scarchilli C, et al. 2016. Meteorological and snow accumulation gradients across Dome C, East Antarctic plateau. *Int J Climatol*, 36(1): 455–466, doi: 10.1002/joc.4362
- Goosse H, Braida M, Crosta X, et al. 2012. Antarctic temperature changes during the last millennium: evaluation of simulations and reconstructions. *Quaternary Sci Rev*, 55: 75–90, doi: 10.1016/j.quascirev.2012.09.003
- Han Y, Huh Y, Hong S, et al. 2011. Quantification of total mercury in Antarctic surface snow using ICP-SF-MS: spatial variation from the coast to dome Fuji. *Bull Korean Chem Soc*, 32(12): 4258–4264, doi: 10.5012/bkcs.2011.32.12.4258
- Hastings M G, Jarvis J C, Steig E J. 2009. Anthropogenic impacts on nitrogen isotopes of ice-core nitrate. *Science*, 324(5932): 1288, doi: 10.1126/science.1170510
- Hastings M G. 2010. Evaluating source, chemistry and climate change based upon the isotopic composition of nitrate in ice cores. *IOP Conf: Ser Earth Environ Sci*, 9(1): 012002
- Hou S G, Li Y S, Xiao C D, et al. 2007. Recent accumulation rate at Dome A, Antarctica. *Chin Sci Bull*, 52(3): 428–431, doi: 10.1007/s11434-007-0041-3
- Hou S G, Li Y S, Xiao C D, et al. 2009. Preliminary results of the close-off depth and the stable isotopic records along a 109.91 m ice core from Dome A, Antarctica. *Sci China Ser D: Earth Sci*, 52(10): 1502–1509, doi: 10.1007/s11430-009-0039-6
- Hou S G, Wang Y T, Pang H X. 2013. Climatology of stable isotopes in Antarctic snow and ice: current status and prospects. *Chin Sci Bull*, 58(10): 1095–1106, doi: 10.1007/s11434-012-5543-y
- Hua R, Hou S, Li Y, et al. 2016. Arsenic record from a 3 m snow pit at Dome Argus, Antarctica. *Antarct Sci*, 28(4): 305–312, doi: 10.1017/S0954102016000092
- Jiang S, Cole-Dai J, Li Y S, et al. 2012. A detailed 2840 year record of explosive volcanism in a shallow ice core from Dome A, East Antarctica. *J Glaciol*, 58(207): 65–75, doi: 10.3189/2012JoG11J138
- Jouzel J, Merlivat L. 1984. Deuterium and oxygen 18 in precipitation: modeling of the isotopic effects during snow formation. *J Geophys Res*, 89(D7): 11749–11757, doi: 10.1029/JD089iD07p11749
- Jouzel J, Masson-Delmotte V, Cattani O, et al. 2007. Orbital and millennial Antarctic climate variability over the past 800,000 years. *Science*, 317(5839): 793–796, doi: 10.1126/science.1141038
- Kawamura K, Abe-Ouchi A, Motoyama H, et al. 2017. State dependence of climatic instability over the past 720,000 years from Antarctic ice cores and climate modeling. *Sci Adv*, 3(2): e1600446, doi: 10.1126/sciadv.1600446
- Kreutz K J, Mayewski P A. 1999. Spatial variability of Antarctic surface snow glaciochemistry: implications for palaeoatmospheric circulation reconstructions. *Antarctic Science*, 11(1): 101–105, doi: 10.1017/S0954102099000140
- Landais A, Barkan E, Luz B. 2008. Record of δ¹⁸O and ¹⁷O-excess in ice from Vostok Antarctica during the last 150,000 years. *Geophys Res Lett*, 35(23): L02709, doi: 10.1029/2008GL034694
- Legrand M, Mayewski P. 1997. Glaciochemistry of polar ice cores: a review. *Rev Geophys*, 35(3): 219–243, doi: 10.1029/96RG03527
- Legrand M, Pasteur E C. 1998. Methane sulfonic acid to non-sea-salt sulfate ratio in coastal Antarctic aerosol and surface snow. *J Geophys Res*, 103(D9): 10991–11006, doi: 10.1029/98JD00929
- Legrand M R, Kirchner S. 1988. Origins and variations of nitrate in polar precipitation. *Chem Geol*, 70(1–2): 101, doi: 10.1016/0009-2541(88)90486-X
- Li C, Kang S, Shi G, et al. 2014. Spatial and temporal variations of total mercury in Antarctic snow along the transect from Zhongshan Station to Dome A. *Tellus B: Chem Phys Meteorol*, 66(1): 25152, doi: 10.3402/tellusb.v66.25152
- Li C J, Xiao C D, Hou S G, et al. 2012. Dating a 109.9 m ice core from Dome A (East Antarctica) with volcanic records and a firm densification model. *Sci China Earth Sci*, 55(8): 1280–1288, doi: 10.1007/s11430-012-4393-4
- Li C, Xiao C, Shi G, et al. 2015. Spatiotemporal variations of monocarboxylic acids in snow layers along a transect from Zhongshan Station to Dome A, eastern Antarctica. *Atmos Res*, 158–159: 79–87, doi: 10.1016/j.atmosres.2015.02.008
- Li C, Xiao C, Shi G, et al. 2016. Spatial and temporal variability of marine-origin matter along a transect from Zhongshan Station to Dome A, eastern Antarctica. *J Environ Sci*, 46: 190–202, doi: 10.1016/j.jes.2015.07.011
- Li Y S, Zhang N, An C L, et al. 2016. Recent progress on Chinese deep ice-core drilling project at Dome A//Second Open Science Conference on International Partnerships in Ice Core Sciences. Hobart, Australia:

IPICS, 232

- Ma T, Xie Z, Li Y, et al. 2017. The spatial changes and impact factors of water stable isotope in surface snow along Zhongshan Station–Dome A. *Chin J Polar Res*, 29(2): 210–217. (in Chinese)
- Ma Y, Bian L, Xiao C, et al. 2010. Near surface climate of the traverse route from Zhongshan Station to Dome A, East Antarctica. *Antarct Sci*, 22(4): 443–459, doi: 10.1017/S0954102010000209
- Masson-Delmotte V, Hou S, Ekaykin A, et al. 2008. A review of Antarctic surface snow isotopic composition: observations, atmospheric circulation, and isotopic modeling. *J Climate*, 21(13): 3359–3387, doi: 10.1175/2007JCL12139.1
- Merlivat L, Jouzel J. 1979. Global climatic interpretation of the deuterium-oxygen 18 relationship for precipitation. *J Geophys Res*, 84(C8): 5029–5033, doi: 10.1029/JC084iC08p05029
- Pang H, Hou S, Landais, et al. 2015. Spatial distribution of ^{17}O -excess in surface snow along a traverse from Zhongshan station to Dome A, East Antarctica. *Earth Planet Sci Lett*, 414: 126–133, doi: 10.1016/j.epsl.2015.01.014
- Petit J, Jouzel J, Raynaud D, et al. 1999. Climate and atmospheric history of the past 420,000 years from the Vostok ice core, Antarctica. *Nature*, 399(6735): 429–436, doi: 10.1038/20859
- Ren J W, Xiao C D, Hou S G, et al. 2009. New focuses of polar ice-core study: NEEM and Dome A. *Chin Sci Bull*, 54(6): 1009–1011, doi: 10.1007/s11434-009-0012-y
- Risi C, Landais A, Bony S, et al. 2010. Understanding the ^{17}O excess glacial–interglacial variations in Vostok precipitation. *J Geophys Res*, 115(D10): D10112
- Röthlisberger R, Hutterli M A, Sommer S, et al. 2000. Factors controlling nitrate in ice cores: evidence from the Dome C deep ice core. *J Geophys Res*, 105(D16): 20565–20572, doi: 10.1029/2000JD900264
- Schneider D P, Noone D C. 2007. Spatial covariance of water isotope records in a global network of ice cores spanning twentieth-century climate change. *J Geophys Res*, 112(D18): D18105, doi: 10.1029/2007JD008652
- Shi G, Buffen A M, Hastings M G, et al. 2014. Investigation of post-depositional processing of nitrate in East Antarctic snow: isotopic constraints on photolytic loss, re-oxidation, and source inputs. *Atmos Chem Phys Discuss*, 14(23): 31943–31986, doi: 10.5194/acpd-14-31943-2014-supplement
- Sun B, Siegert M J, Mudd S M, et al. 2009. The Gamburtsev mountains and the origin and early evolution of the Antarctic Ice Sheet. *Nature*, 459(7247): 690–693, doi: 10.1038/nature08024
- Talbot R W, Beecher K M, Harriss R C, et al. 1988. Atmospheric geochemistry of formic and acetic acids at a mid-latitude temperate site. *J Geophys Res*, 93(D2): 1638–1652, doi: 10.1029/JD093iD02p01638
- Uemura R, Barkan E, Abe O, et al. 2010. Triple isotope composition of oxygen in atmospheric water vapor. *Geophys Res Lett*, 37(4): L04402, doi: 10.1029/2009GL041960
- Vimeux F, Masson V, Delaygue G, et al. 2001. A 420,000 year deuterium excess record from East Antarctica: information on past changes in the origin of precipitation at Vostok. *J Geophys Res*, 106(D23): 31863–31873, doi: 10.1029/2001JD900076
- Wang T, Sun B, Tang X, et al. 2016. Spatio-temporal variability of past accumulation rates inferred from isochronous layers at Dome A, East Antarctica. *Ann Glaciol*, 57(73): 87–93, doi: 10.1017/aog.2016.28
- Wang Y, Hou S, Masson-Delmotte V, et al. 2009. A new spatial distribution map of $\delta^{18}\text{O}$ in Antarctic surface snow. *Geophys Res Lett*, 36(6): L06501, doi: 10.1029/2008GL036939
- Wang Y, Sodemann H, Hou S, et al. 2013. Snow accumulation and its moisture origin over Dome Argus, Antarctica. *Climate Dyn*, 40(3–4): 731–742, doi: 10.1007/s00382-012-1398-9
- Wolff E W. 1995. Nitrate in polar ice//Delmas R J. Ice core studies of global biogeochemical cycles. Berlin, Heidelberg: Springer, 195–224
- Xiao C, Ding M, Masson-Delmotte V, et al. 2013. Stable isotopes in surface snow along a traverse route from Zhongshan station to Dome A, East Antarctica. *Climate Dyn*, 41(9–10): 2427–2438, doi: 10.1007/s00382-012-1580-0
- Xiao C, Li Y, Allison I, et al. 2008. Surface characteristics at Dome A, Antarctica: first measurements and a guide to future ice-coring sites. *Ann Glaciol*, 48: 82–87, doi: 10.3189/172756408784700653
- Xiao C D, Li Y S, Hou S G, et al. 2008. Preliminary evidence indicating Dome A (Antarctica) satisfying preconditions for drilling the oldest ice core. *Chin Sci Bull*, 53(1): 102–106, doi: 10.1007/s11434-007-0520-6
- Yan P, Hou S, Chen T, et al. 2012. Culturable bacteria isolated from snow cores along the 1300 km traverse from Zhongshan Station to Dome A, East Antarctica. *Extremophiles*, 16(2): 345–354, doi: 10.1007/s00792-012-0434-3
- Yang Y, Sun B, Wang Z, et al. 2014. GPS-derived velocity and strain fields around Dome Argus, Antarctica. *J Glaciol*, 60(222): 735–742, doi: 10.3189/2014JoG14J078
- Zhang N, An C, Fan X, et al. 2014. Chinese first deep ice-core drilling project DK-1 at Dome A, Antarctica (2011–2013): progress and performance. *Ann Glaciol*, 55(68): 88–98, doi: 10.3189/2014AoG68A006
- Zhang S, E D, Wang Z, et al. 2007. Surface topography around the summit of Dome A, Antarctica, from real-time kinematic GPS. *J Glaciol*, 53(180): 159–160, doi: 10.3189/172756507781833965